

Kinetic Theory of Binary Granular Suspensions at Low Density. Thermal Diffusion Segregation



Rubén Gómez González and Vicente Garzó

Abstract Transport properties of granular mixtures surrounded by an interstitial gas are determined by solving the Boltzmann kinetic equation by means of the Chapman–Enskog method. As usual, the influence of the viscous gas on solid particles is accounted for by an effective external force composed of two terms: a drag force proportional to the particle velocity plus a stochastic Langevin-like term. Before considering inhomogeneous situations, we study first the homogeneous steady state where collisional cooling and viscous friction are compensated for by the energy gained by grains due to their interaction with the interstitial gas. Then, the Chapman–Enskog method is used to solve the Boltzmann equation and express the Navier–Stokes transport coefficients in terms of the solutions of a set of coupled linear integral equations. Explicit forms are obtained here in the tracer limit for the diffusion transport coefficients which are explicitly determined by considering the so-called first Sonine approximation. As an application of the previous results, thermal diffusion segregation of an intruder immersed in a granular suspension is analyzed and compared with previous theoretical attempts where the effect of the interstitial gas was neglected.

1 Introduction

Granular matter in nature is generally surrounded by an interstitial fluid, like water or air. Although in many situations the effect of the surrounding fluid on the dynamic properties of grains can be neglected, there are also other situations (for instance, when the stress exerted by the fluid phase on grains is significant) where the influence of the interstitial fluid must necessarily be taken into account. A typical example of it refers to the species segregation in granular mixtures [1]. Since a granular suspension is a multiphase process, in the context of kinetic theory, one could start from a set of coupled kinetic equations for each one of the velocity distribution functions of the

R. Gómez González · V. Garzó (✉)
Departamento de Física and Instituto de Computación Científica Avanzada (ICCAEx),
Universidad de Extremadura, 06006 Badajoz, Spain
e-mail: vicenteg@unex.es

© The Author(s), under exclusive license to Springer Nature Switzerland AG 2022
L. Brenig et al. (eds.), *Nonequilibrium Thermodynamics and Fluctuation Kinetics*,
Fundamental Theories of Physics 208,
https://doi.org/10.1007/978-3-031-04458-8_9

phases. However, this approach involves many technical intricacies, especially in the case of granular mixtures. Thus, to avoid this problem, the effect of the interstitial fluid on grains is usually taken into account by means of an effective external force [2]. This fluid–solid force is composed of two terms: (i) a viscous drag force (Stokes’ law) proportional to the particles velocity and (ii) a stochastic force modeled as a Gaussian white noise. While the first term mimics the friction of grains with the surrounding gas, the second term accounts for the energy gained by grains due to their interaction with the particles of the gas phase (thermal reservoir).

An interesting and challenging problem is to assess the impact of gas phase on the Navier–Stokes transport coefficients of a binary granular mixture modeled as an ensemble of smooth inelastic hard spheres. This problem is not only relevant from a fundamental point of view but also from a realistic point of view since granular suspensions are present in nature formed by grains of different masses, sizes, densities, and coefficients of restitution. However, the determination of the transport coefficients of bidisperse gas–solid flows is a quite ambitious target due essentially to the large number of integro–differential equations involved as well as the wide parameter space of the system. For this reason and in order to offer a complete description, we consider here binary granular suspensions at low-density where the Boltzmann kinetic equation turns out to be a reliable starting point [3, 4].

As in previous papers [6–8], the Boltzmann equation (BE) is solved by means of the Chapman–Enskog (CE) method [9] adapted to dissipative dynamics. A subtle and important point of the expansion method is the choice of the reference distribution in the perturbation scheme. Although we are interested here in obtaining the transport coefficients under steady conditions, the presence of the surrounding fluid gives rise to a local energy unbalance in such a way the zeroth-order distributions $f_i^{(0)}$ of each species (reference states) are not in general stationary distributions. Thus, in order to determine the Navier–Stokes transport coefficients, one has to obtain first the unsteady integral equations defining the above transport coefficients and solve (approximately) then these equations in steady-state conditions. An important consequence of this procedure is that the transport properties depend not only on the steady temperature but also on quantities such as the derivatives of the temperature ratio on the temperature.

The plan of the paper is as follows. The granular suspension model as well as the balance equations for the densities of mass, momentum, and energy are derived in Sect. 2. Then, the steady homogeneous state is studied in Sect. 3 where the temperature ratio T_1/T_2 of both species is calculated and compared against the Monte Carlo simulations. Section 4 addresses the application of the CE method up to first order in the spatial gradients. As expected, transport coefficients are given in terms of the solutions of a set of coupled linear integral equations. These integral equations are approximately solved by considering the leading Sonine approximation; this procedure is explicitly displayed here for the diffusion transport coefficients in the special limit case where one of the components of the mixture is present in tracer concentration. As an application of the previous results, thermal diffusion segregation of an intruder or tracer particle is analyzed in Sect. 5. The paper is closed in Sect. 6 with a brief discussion of the results obtained in this work.

2 Granular Suspension Model

We consider a granular binary mixture of inelastic hard disks ($d = 2$) or spheres ($d = 3$) of masses m_i and diameters σ_i ($i = 1, 2$). The spheres are assumed to be completely smooth and so, the inelasticity of collisions is characterized by three constant (positive) coefficients of normal restitution $\alpha_{ij} \leq 1$. The solid particles are surrounded by a molecular gas of viscosity η_g and temperature T_{ex} . As said before, the influence of the interstitial gas on grains is modeled via a fluid–solid force constituted by two terms: a deterministic drag force plus a stochastic force. In the low-density limit and taking into account the above terms, the one-particle velocity distribution function of each species verifies the Boltzmann kinetic equation [8]

$$\frac{\partial f_i}{\partial t} + \mathbf{v} \cdot \nabla f_i - \gamma_i \Delta \mathbf{U} \cdot \frac{\partial f_i}{\partial \mathbf{v}} - \gamma_i \frac{\partial}{\partial \mathbf{v}} \cdot \mathbf{v} f_i - \frac{\gamma_i T_{ex}}{m_i} \frac{\partial^2 f_i}{\partial v^2} = \sum_{j=1}^2 J_{ij}[f_i, f_j], \quad (1)$$

where $J_{ij}[f_i, f_j]$ is the Boltzmann collision operator [4]. In addition, $\Delta \mathbf{U} = \mathbf{U} - \mathbf{U}_g$, $\mathbf{V} = \mathbf{v} - \mathbf{U}$ is the peculiar velocity,

$$\mathbf{U} = \rho^{-1} \sum_{i=1}^2 \int d\mathbf{v} m_i \mathbf{v} f_i(\mathbf{v}) \quad (2)$$

is the mean flow velocity of the solid particles, and \mathbf{U}_g is the known mean flow velocity of the interstitial gas. The friction coefficients γ_i are proportional to the gas viscosity η_g and are functions of the partial volume fractions $\phi_i = (\pi^{d/2}/(2^{d-1}d\Gamma(d/2)))n_i\sigma_i^d$, where

$$n_i = \int d\mathbf{v} f_i(\mathbf{v}) \quad (3)$$

is the number density of species i . In the dilute limit, every particle is only subjected to its respective Stokes' drag [10] so that for hard spheres ($d = 3$) γ_i is

$$\gamma_i = \gamma_0 R_i, \quad \gamma_0 = \frac{18\eta_g}{\rho\sigma_{12}^2}, \quad R_i = \frac{\rho\sigma_{12}^2}{\rho_i\sigma_i^2}\phi_i. \quad (4)$$

Here, $\rho_i = m_i n_i$, $\rho = \rho_1 + \rho_2$ is the total mass density, and $\sigma_{12} = (\sigma_1 + \sigma_2)/2$. Apart from the partial densities n_i and the mean flow velocity \mathbf{U} , the other relevant hydrodynamic field is the granular temperature T , defined as

$$T = \frac{1}{n} \sum_{i=1}^2 \int d\mathbf{v} \frac{m_i}{d} V^2 f_i(\mathbf{v}), \quad (5)$$

where $n = n_1 + n_2$ is the total number density.

The Boltzmann collision operators $J_{ij}[f_i, f_j]$ conserve the number densities of each species and the total momentum but the total energy is not conserved:

$$\int d\mathbf{v} \left\{ 1, \sum_{i,j} m_i \mathbf{v}, \sum_{i,j} m_i V^2 \right\} J_{ij}[\mathbf{v}|f_i, f_j] = \{0, \mathbf{0}, -dnT\zeta\}, \quad (6)$$

where ζ is the total cooling rate due to inelastic collisions among all species. The macroscopic balance equations for the densities of mass, momentum, and energy can be easily obtained by multiplying both sides of the BE (1) by 1, $m_i \mathbf{v}$, and $m_i V^2$; integrating over \mathbf{v} ; and taking into account the properties (6). After some algebra, one gets

$$D_t n_i + n_i \nabla \cdot \mathbf{U} + \frac{\nabla \cdot \mathbf{j}_i}{m_i} = 0, \quad (7)$$

$$D_t \mathbf{U} + \rho^{-1} \nabla \cdot \mathbf{P} = -\rho^{-1} \Delta \mathbf{U} \sum_{i=1}^2 \rho_i \gamma_i - \rho^{-1} (\gamma_1 - \gamma_2) \mathbf{j}_1, \quad (8)$$

$$\begin{aligned} D_t T - \frac{T}{n} \sum_{i=1}^2 \frac{\nabla \cdot \mathbf{j}_i}{m_i} + \frac{2}{dn} (\nabla \cdot \mathbf{q} + \mathbf{P} : \nabla \mathbf{U}) = -\frac{2}{dn} \Delta \mathbf{U} \cdot \sum_{i=1}^2 \gamma_i \mathbf{j}_i \\ + 2 \sum_{i=1}^2 x_i \gamma_i (T_{\text{ex}} - T_i) - \zeta T. \end{aligned} \quad (9)$$

In the above equations, $D_t = \partial_t + \mathbf{U} \cdot \nabla$ is the material derivative,

$$\mathbf{j}_i = m_i \int d\mathbf{v} \mathbf{V} f_i(\mathbf{v}) \quad (\mathbf{j}_1 = -\mathbf{j}_2) \quad (10)$$

is the mass flux for the component i relative to the local flow \mathbf{U} ,

$$\mathbf{P} = \sum_{i=1}^2 \int d\mathbf{v} m_i \mathbf{V} \mathbf{V} f_i(\mathbf{v}) \quad (11)$$

is the pressure tensor, and

$$\mathbf{q} = \sum_{i=1}^2 \int d\mathbf{v} \frac{m_i}{2} V^2 \mathbf{V} f_i(\mathbf{v}) \quad (12)$$

is the heat flux. In addition, the partial kinetic temperature T_i is

$$T_i = \frac{m_i}{dn_i} \int d\mathbf{v} V^2 f_i(\mathbf{v}). \quad (13)$$

The partial temperature T_i measures the mean kinetic energy of particles of species i . The relationship between the granular temperature T and the partial temperatures T_i is simply given by $T = \sum_i x_i T_i$, where $x_i = n_i/n$ is the concentration of species i . The breakdown of energy equipartition in granular systems ($T_i \neq T$) predicted by kinetic theory [4] has been confirmed in computer simulations [11] as well as in real experiments [12].

It is quite apparent that the balance equations (7)–(9) become a closed set of differential equations for n_1 , n_2 , \mathbf{U} , and T when the fluxes, the cooling rate, and the partial temperatures are expressed in terms of the hydrodynamic fields and their gradients. These constitutive equations for \mathbf{j}_i , \mathbf{P} , \mathbf{q} , ζ , and T_i may be derived by solving the BE (1) by the CE expansion up to first order in spatial gradients. This will be analyzed in Sect. 4.

3 Homogeneous Steady States

As a first step and before studying inhomogeneous situations, we consider homogeneous states. In this case, n_i and T are spatially uniform, and with a convenient choice of the reference frame, the mean velocities vanish ($\mathbf{U} = \mathbf{U}_g = \mathbf{0}$). For times longer than the mean free time, it is expected that the suspension achieves a steady state ($\partial_t f_i = 0$) where the BE (1) reads

$$-\gamma_i \frac{\partial}{\partial \mathbf{v}} \cdot \mathbf{v} f_i - \frac{\gamma_i T_{\text{ex}}}{m_i} \frac{\partial^2 f_i}{\partial v^2} = \sum_{j=1}^2 J_{ij}[f_i, f_j]. \quad (14)$$

The balance equation for the partial temperature T_i can be easily derived by multiplying both sides of Eq. (14) by $m_i v^2$ and integrating over velocity:

$$2\gamma_i (T_{\text{ex}} - T_i) = \zeta_i T_i, \quad (15)$$

where the partial cooling rates ζ_i for the partial temperatures T_i are defined as

$$\zeta_i = -\frac{m_i}{dn_i T_i} \sum_{j=1}^2 \int d\mathbf{v} v^2 J_{ij}[f_i, f_j], \quad (i = 1, 2). \quad (16)$$

The relationship between ζ and ζ_i is

$$\zeta = \sum_{i=1}^2 x_i \tau_i \zeta_i, \quad (17)$$

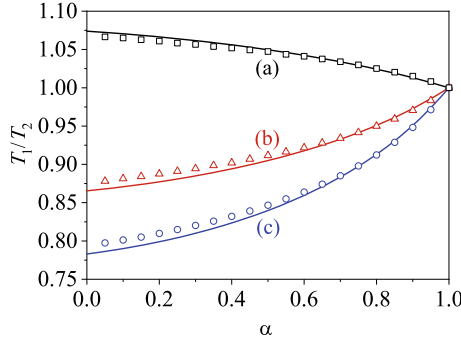


Fig. 1 Temperature ratio T_1/T_2 versus the (common) coefficient of restitution α for $d = 3$, $x_1 = 0.5$, $\sigma_1/\sigma_2 = 1$, $T_{\text{ex}}^* = 1$, and three different values of the mass ratio: $m_1/m_2 = 0.5$ (a), $m_1/m_2 = 4$ (b), and $m_1/m_2 = 10$ (c). Lines are the theoretical results while symbols refer to the Monte Carlo simulations

where $\tau_i = T_i/T$ is the temperature ratio of the species i . Upon deriving Eq. (17), use has been made of the relation $T = \sum_i x_i T_i$ and Eq. (6).

For elastic collisions ($\alpha_{ij} = 1$), $\zeta = \zeta_i = 0$, Eq. (15) yields $T_i = T_{\text{ex}} = T$ so that the Maxwellian distribution with a common temperature is a solution of the BE (14). On the other hand, for inelastic collisions ($\alpha_{ij} \neq 1$), ζ_i and ζ are different from zero and to date the solution to Eq. (14) is unknown. Thus, one has to consider an approximate form for the distributions f_i to estimate ζ_i . Here, we take the simplest approximation for both distributions, namely the Maxwellian distributions $f_{i,M}$ defined with the partial temperatures T_i :

$$f_i(\mathbf{v}) \rightarrow f_{i,M}(\mathbf{v}) = n_i \left(\frac{m_i}{2\pi T_i} \right)^{d/2} \exp\left(-\frac{m_i v^2}{2T_i} \right). \quad (18)$$

The partial cooling rates can be computed from Eq. (16) by replacing f_i by $f_{i,M}$. The result is [4]

$$\begin{aligned} \zeta_1 = & \frac{\sqrt{2}\pi^{(d-1)/2}}{d\Gamma\left(\frac{d}{2}\right)} n_1 \sigma_1^{d-1} \left(\frac{2T_1}{m_1} \right)^{1/2} (1 - \alpha_{11}^2) + \frac{4\pi^{(d-1)/2}}{d\Gamma\left(\frac{d}{2}\right)} n_2 \sigma_{12}^{d-1} \mu_{21} \\ & \times \left(\frac{2T_1}{m_1} + \frac{2T_2}{m_2} \right)^{1/2} (1 + \alpha_{12}) \left[1 - \frac{\mu_{21}}{2} (1 + \alpha_{12}) \left(1 + \frac{m_1 T_2}{m_2 T_1} \right) \right], \quad (19) \end{aligned}$$

where $\mu_{ij} = m_i/(m_i + m_j)$. The expression for ζ_2 can be easily obtained from Eq. (19) by making the change $1 \leftrightarrow 2$.

The partial temperatures T_i can be obtained from Eq. (15) (for $i = 1, 2$) when the expressions (19) for ζ_1 and ζ_2 are considered. Figure 1 plots the temperature ratio T_1/T_2 as a function of the (common) coefficient of restitution $\alpha \equiv \alpha_{ij}$ for $x_1 = 0.5$, $\sigma_1 = \sigma_2$, $T_{\text{ex}}^* = 1$, and three different values of the mass ratio. Here,

$T_{\text{ex}}^* = T_{\text{ex}}/(\bar{m}\sigma_{12}^2\gamma_0^2)$ and $\bar{m} = (m_1 + m_2)/2$. Theory is compared against the Monte Carlo simulations [13]. As expected, energy equipartition is broken for inelastic collisions; the extent of the energy violation is greater when the mass disparity is large. The excellent agreement found between theory and computer simulations is also quite apparent, except for quite small values of α (extreme inelasticity) where small discrepancies appear.

4 Chapman–Enskog Method. First-Order Solution

We assume now that the homogeneous steady state is perturbed by small spatial gradients. The existence of these gradients gives rise to nonzero contributions to the fluxes of mass, momentum, and energy. To first order in spatial gradients, the knowledge of the above fluxes allows one to identify the relevant Navier–Stokes transport coefficients of the granular suspension. As usual in the CE scheme [9], for times longer than the mean free time and distances larger than the mean free path, we suppose that the system achieves a hydrodynamic regime. This means that (i) the system has completely “forgotten” its initial preparation (initial conditions) and (ii) only the bulk domain of the system (namely, far away from the boundaries) is considered. Under these conditions, the BE (1) admits a special solution: the so-called *normal* or hydrodynamic solution where all space and time dependence of the distributions $f_i(\mathbf{r}, \mathbf{v}; t)$ is through a functional dependence on the hydrodynamic fields. This means that in the hydrodynamic regime, $f_i(\mathbf{r}, \mathbf{v}; t)$ adopts the normal form

$$f_i(\mathbf{r}, \mathbf{v}; t) = f_i[\mathbf{v}|n_1(t), n_2(t), T(t), \mathbf{U}(t)]. \quad (20)$$

The notation on the right-hand side of Eq. (20) indicates a functional dependence on the partial densities, temperature, and flow velocity. For small Knudsen numbers, the functional dependence (20) can be made local in space by expanding f_i in powers of the spatial gradients

$$f_i = f_i^{(0)} + \epsilon f_i^{(1)} + \epsilon^2 f_i^{(2)} + \dots, \quad (21)$$

where ϵ is a bookkeeping parameter that denotes an implicit spatial gradient (for instance, a term of order ϵ is of first order in gradients). This parameter is taken to be equal to 1 at the end of the calculations.

An important point in the CE expansion is to characterize the magnitude of the friction coefficients γ_i and the term $\Delta\mathbf{U}$ with respect to the spatial gradients. On the one hand, since γ_i does not create any flux, then it is assumed to be to zeroth order in ϵ . On the other hand, because $\Delta\mathbf{U} = \mathbf{0}$ in the absence of gradients, it should be considered to be at least of first order in spatial gradients (first order in ϵ).

The implementation of the CE method to solve the BE (1) to first order in spatial gradients is very large and beyond the scope of the present contribution. We refer the interested reader to Ref. [8] for specific details. Since we want here to analyze

thermal diffusion segregation in a granular suspension, in order to show more clearly the different competing mechanisms appearing in this phenomenon, we consider a binary mixture where the concentration of one of the species (let's say species 1) is much smaller than that of the other species 2 (tracer limit, $x_1 \rightarrow 0$). The consideration of this simple situation allows us to offer a simplified theory where a segregation criterion can be explicitly obtained.

In the tracer limit, the pressure tensor P_{ij} , the heat flux \mathbf{q} , and the cooling rate ζ of the binary mixture are the same as that of the excess species. While the fluxes P_{ij} and \mathbf{q} are of first order in the spatial gradients in the Navier–Stokes description, the expression of ζ must retain terms up to second order in gradients. Part of these second-order contributions to ζ have been computed by Brey et al. [5] for dry (dilute) granular gases, while the complete set of these contributions has been determined by Brilliantov and Pöschel [14] for granular gases of viscoelastic particles. Nevertheless, it has been shown [5] that these second-order contributions to ζ are negligible as compared with its zeroth-order counterparts. We expect that the same occurs for the case of binary granular suspensions and hence, they can be ignored.

4.1 Tracer Limit. Diffusion Transport Coefficients

In the tracer limit, the first-order contribution $\mathbf{j}_1^{(1)}$ to the mass flux is [8]

$$\mathbf{j}_1^{(1)} = -\frac{m_1^2}{\rho} D_{11} \nabla n_1 - \frac{m_1 m_2}{\rho} D_{12} \nabla n_2 - \frac{\rho}{T} D_1^T \nabla T - D_1^U \Delta \mathbf{U}, \quad (22)$$

where the diffusion transport coefficients are defined as

$$D_{11} = -\frac{\rho}{\rho_1 d} \int d\mathbf{v} \mathbf{V} \cdot \mathcal{B}_{11}(\mathbf{V}), \quad D_{12} = -\frac{1}{d} \int d\mathbf{v} \mathbf{V} \cdot \mathcal{B}_{12}(\mathbf{V}), \quad (23)$$

$$D_1^T = -\frac{m_1}{\rho d} \int d\mathbf{v} \mathbf{V} \cdot \mathcal{A}_1(\mathbf{V}), \quad D_1^U = -\frac{m_1}{d} \int d\mathbf{v} \mathbf{V} \cdot \mathcal{E}_1(\mathbf{V}). \quad (24)$$

The unknowns $\mathcal{A}_1(\mathbf{V})$, $\mathcal{B}_{11}(\mathbf{V})$, $\mathcal{B}_{12}(\mathbf{V})$, and $\mathcal{E}_1(\mathbf{V})$ are the solutions of a set of coupled linear integral equations [8]. In the tracer limit, this set reads

$$\begin{aligned} -\left(2\gamma_2\theta^{-1} + \frac{1}{2}\zeta^{(0)}\right)\mathcal{A}_1 - \gamma_1 \frac{\partial}{\partial \mathbf{V}} \cdot (\mathbf{V}\mathcal{A}_1) - \gamma_1 \frac{T_{\text{ex}}}{m_1} \frac{\partial^2 \mathcal{A}_1}{\partial v^2} - J_{12}[\mathcal{A}_1, f_2^{(0)}] \\ = \mathbf{A}_1 + J_{12}[f_1^{(0)}, \mathcal{A}_2], \end{aligned} \quad (25)$$

$$-\gamma_1 \frac{\partial}{\partial \mathbf{V}} \cdot (\mathbf{V}\mathcal{B}_{11}) - \gamma_1 \frac{T_{\text{ex}}}{m_1} \frac{\partial^2 \mathcal{B}_{11}}{\partial v^2} - J_{12}[\mathcal{B}_{11}, f_1^{(0)}] = \mathbf{B}_{11}, \quad (26)$$

$$\begin{aligned}
-\gamma_1 \frac{\partial}{\partial \mathbf{V}} \cdot (\mathbf{V} \mathcal{B}_{12}) - \gamma_1 \frac{T_{\text{ex}}}{m_1} \frac{\partial^2 \mathcal{B}_{12}}{\partial v^2} - J_{12}[\mathcal{B}_{12}, f_2^{(0)}] = \mathbf{B}_{12} + J_{12}[f_1^{(0)}, \mathcal{B}_{21}] \\
+ \left[\zeta^{(0)} - 2\gamma_2 (\theta^{-1} - 1) + 2\lambda_1 \frac{\partial \tau_1}{\partial \lambda_1} \right] \mathcal{A}_1, \quad (27)
\end{aligned}$$

$$-\gamma_1 \frac{\partial}{\partial \mathbf{V}} \cdot (\mathbf{V} \mathcal{E}_1) - \gamma_1 \frac{T_{\text{ex}}}{m_1} \frac{\partial^2 \mathcal{E}_1}{\partial v^2} - J_{12}[\mathcal{E}_1, f_2^{(0)}] = \mathbf{E}_1. \quad (28)$$

In the integral equations (25)–(28), $\zeta^{(0)}$ is the zeroth-order approximation to the cooling rate, $\theta = T/T_{\text{ex}}$, $\lambda_1 = (2T_{\text{ex}}^*)^{-1/2} (R_1/n\sigma_{12}^d)$, and \mathcal{A}_2 and \mathcal{B}_{21} refer to quantities of the excess species 2. These quantities obey certain integral equations; their explicit forms are not needed for evaluating the diffusion transport coefficients in the so-called first Sonine approximation. In addition, the expression of the derivative $\partial_{\lambda_1} \tau_1$ can be found in Appendix A of Ref. [8] while the inhomogeneous terms \mathcal{A}_1 , \mathbf{B}_{11} , \mathbf{B}_{12} , and \mathbf{E}_1 are given, respectively, by

$$\mathbf{A}_1(\mathbf{V}) = -\mathbf{V} \frac{\partial f_1^{(0)}}{\partial T} - \frac{p}{\rho} \frac{\partial f_1^{(0)}}{\partial \mathbf{V}}, \quad \mathbf{B}_{11}(\mathbf{V}) = -\mathbf{V} n_1 \frac{\partial f_1^{(0)}}{\partial n_1}, \quad (29)$$

$$\mathbf{B}_{12}(\mathbf{V}) = -\mathbf{V} n_2 \frac{\partial f_1^{(0)}}{\partial n_2} - \frac{T}{m_2} \frac{\partial f_1^{(0)}}{\partial \mathbf{V}}, \quad \mathbf{E}_1(\mathbf{V}) = (\gamma_1 - \gamma_2) \frac{\partial f_1^{(0)}}{\partial \mathbf{V}}. \quad (30)$$

Note that Eqs. (25)–(28) have been obtained under steady-state conditions, namely when the conditions (15) apply. Furthermore, in order to obtain the above set of coupled integral equations, we have taken into account that while in the tracer limit D_{11} is independent of x_1 , the coefficients D_{12} , D_1^T , and D_1^U are proportional to x_1 . This dependence on x_1 will be then self-consistently confirmed. Accordingly, $\mathcal{A}_1 \propto x_1$, $\mathcal{B}_{12} \propto x_1$, and $\mathcal{E}_1 \propto x_1$.

Although the exact form of the zeroth-order distributions $f_i^{(0)}$ is not known, dimensional analysis requires that they have the scaled form $f_i^{(0)}(\mathbf{V}) = n_i v_{\text{th}}^{-d} \varphi_i(\mathbf{c}, \gamma_i^*, \theta)$. Here, $\mathbf{c} = \mathbf{V}/v_{\text{th}}$ and $\gamma_i^* = \gamma_i/\nu_0$, where $\nu_0 = n\sigma_{12}^{d-1} v_{\text{th}}$ is an effective collision frequency, and $v_{\text{th}} = \sqrt{2T/\bar{m}}$ is the thermal velocity. Thus, one has the property

$$T \frac{\partial f_i^{(0)}}{\partial T} = -\frac{1}{2} \frac{\partial}{\partial \mathbf{V}} \cdot \mathbf{V} f_i^{(0)} + n_i v_{\text{th}}^{-d} \theta \frac{\partial \varphi_i}{\partial \theta}. \quad (31)$$

4.2 Leading Sonine Approximation

Equations (25)–(28) are still exact. However, the determination of the diffusion transport coefficients requires to solve the above integral equations as well as to know

the zeroth-order distributions $f_i^{(0)}$. The results derived for driven granular mixtures [15] have shown that non-Gaussian corrections to $f_i^{(0)}$ (which are measured through the fourth cumulants c_i) are in general very small. Thus, $f_i^{(0)}$ is well represented by its Maxwellian form (18) and so, a theory incorporating the cumulants c_i seems to be unnecessary in practice for computing the diffusion transport coefficients. Regarding the functions \mathcal{A}_i , \mathcal{B}_{ij} , and \mathcal{E}_i , as usual we consider the leading terms in a series expansion of these quantities in Sonine polynomials. In this case, $\mathcal{A}_2 \rightarrow 0$, $\mathcal{B}_{21} \rightarrow 0$, and the quantities \mathcal{A}_1 , \mathcal{B}_{11} , \mathcal{B}_{12} , and \mathcal{E}_1 corresponding to the tracer species are approximated by

$$\mathcal{A}_1(\mathbf{V}) \rightarrow -f_{1,M} \mathbf{V} \frac{\rho}{n_1 T_1} D_1^T, \quad \mathcal{B}_{11}(\mathbf{V}) \rightarrow -f_{1,M} \mathbf{V} \frac{m_1^2}{\rho T_1} D_{11}, \quad (32)$$

$$\mathcal{B}_{12}(\mathbf{V}) \rightarrow -f_{1,M} \mathbf{V} \frac{m_1}{n_1 T_1} D_{12}, \quad \mathcal{E}_1(\mathbf{V}) \rightarrow -f_{1,M} \mathbf{V} \frac{1}{n_1 T_1} D_1^U. \quad (33)$$

Now, we substitute first Eqs. (32) and (33) into the integral equations (25)–(28), multiply them by $m_1 \mathbf{V}$, and integrate over \mathbf{v} . After some algebra, D_{11} , D_1^T , D_{12} , and D_1^U can be written, respectively, as

$$D_{11} = \frac{\rho T}{m_1^2 \nu_0} \frac{\tau_1}{\nu_D^* + \gamma_1^*}, \quad D_1^T = \frac{n T}{\rho \nu_0} x_1 \frac{\theta \frac{\partial \tau_1}{\partial \theta} - (\mu - \tau_1)}{\nu_D^* + \gamma_1^* - 2\gamma_2^* \theta^{-1} - \frac{1}{2} \zeta_0^*}, \quad (34)$$

$$D_{12} = \frac{x_1 \rho T}{m_1 m_2 \nu_0} \frac{[\zeta_0^* - 2\gamma_2^* (\theta^{-1} - 1)] x_1^{-1} D_1^{T*} - \mu - 2\lambda_1 \frac{\partial \tau_1}{\partial \lambda_1}}{\nu_D^* + \gamma_1^*}, \quad (35)$$

$$D_1^U = \rho_1 \frac{\gamma_1^* - \gamma_2^*}{\gamma_1^* - \nu_D^*}. \quad (36)$$

Here, $\mu = m_1/m_2$ is the mass ratio, the derivative $\partial_\theta \tau_1$ is given in Appendix A of Ref. [8],

$$\zeta_0^* = \frac{\pi^{(d-1)/2}}{d\Gamma(\frac{d}{2})} \left(\frac{\sigma_2}{\sigma_{12}}\right)^{d-1} \mu_{21}^{-1/2} (1 - \alpha_{22}^2), \quad (37)$$

and the reduced collision frequency ν_D^* is

$$\nu_D^* = \frac{2\sqrt{2}\pi^{(d-1)/2}}{d\Gamma(\frac{d}{2})} \mu_{21}^{3/2} \left(\frac{1+\beta}{\beta}\right)^{1/2} (1 + \alpha_{12}), \quad (38)$$

where $\beta = \beta_1/\beta_2 = \mu/\tau_1$.

Figure 2 shows the dependence of the reduced diffusion transport coefficients $D_{ij}(\alpha)/D_{ij}(1)$, $D_1^T(\alpha)/D_1^T(1)$, and $D_1^U(\alpha)/D_1^U(1)$ for $\sigma_1/\sigma_2 = 1$, $m_1/m_2 = 10$, and $T_{\text{ex}}^* = 0.1$. Here, $D_{ij}(1)$, $D_1^T(1)$, and $D_1^U(1)$ are the values of these coefficients

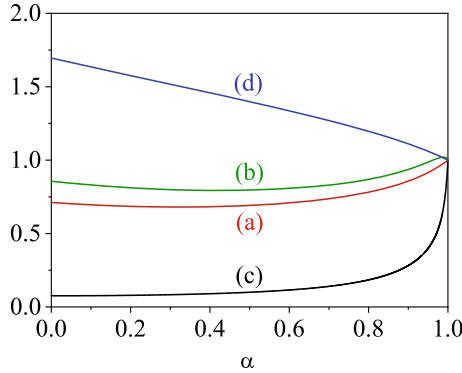


Fig. 2 Plot of the (reduced) transport coefficients $D_{11}(\alpha)/D_{11}(1)$ (a), $D_{12}(\alpha)/D_{12}(1)$ (b), $D_1^T(\alpha)/D_1^T(1)$ (c), and $D_1^U(\alpha)/D_1^U(1)$ (d) as a function of the common coefficient of restitution for a binary mixture of hard spheres ($d = 3$) in the tracer limit ($x_1 \rightarrow 0$) with $\sigma_1/\sigma_2 = 1$, $m_1/m_2 = 10$, and $T_{ex}^* = 0.1$

for elastic collisions. We observe that the impact of inelasticity on those coefficients is in general quite important since they differ clearly from their elastic forms, especially in the case of the thermal diffusion coefficient D_1^T . Moreover, a comparison with the results obtained in the dry granular limit (no gas phase) shows important qualitative differences between both theories (see, for instance, Fig. 6.3 of Ref. [4] for the diffusion coefficient D_{11}).

5 Thermal Diffusion Segregation of an Intruder in a Granular Suspension

A nice application of the previous results is the study of thermal diffusion segregation of an intruder or tracer particle in a granular suspension. Needless to say, segregation and mixing of dissimilar grains are one of the most interesting problems in granular mixtures, not only from a fundamental point of view but also from a more practical perspective. This problem has been widely studied in the past few years for dry granular mixtures. The objective here is to assess the influence of the interstitial gas phase on the segregation criterion.

Thermal diffusion is originated by the relative motion of the components of a mixture due to the presence of a temperature gradient. Due to this motion, concentration gradients appear in the mixture producing ordinary diffusion. A steady state is finally achieved in which the separating effect emerging from thermal diffusion is offset by the remixing effect arising from ordinary diffusion [16]. The partial separation between both components of the mixture is then observed; this effect is usually referred to as the Soret effect.

The amount of segregation parallel to the thermal gradient may be characterized by the so-called thermal diffusion factor Λ . This quantity is defined in an inhomogeneous

non-convecting ($\mathbf{U} = \mathbf{U}_g = \mathbf{0}$) steady state with zero mass flux ($\mathbf{j}_1^{(1)} = \mathbf{0}$) as

$$-\Lambda \frac{\partial \ln T}{\partial z} = \frac{\partial}{\partial z} \ln \left(\frac{n_1}{n_2} \right), \quad (39)$$

where only gradients along the z -axis have been assumed for simplicity. Let us assume that the bottom plate is hotter than the top plate ($\partial_z \ln T < 0$). If Λ is supposed to be constant over the relevant ranges of composition and temperature of the system, according to Eq. (39), when $\Lambda > 0$, the tracer particle tends to rise with respect to the gas particles 2, i.e., $\partial_z \ln(n_1/n_2) > 0$ (tracer particles accumulate near the cold plate). On the other hand, when $\Lambda < 0$, the tracer particle tends to fall with respect to the gas particles 2, i.e., $\partial_z \ln(n_1/n_2) < 0$ (tracer particles accumulate near the hot plate).

Let us determine the thermal diffusion factor. The mass flux $j_{1,z}^{(1)}$ is given by Eq. (22) with $\Delta \mathbf{U} = \mathbf{0}$. Since $j_{1,z}^{(1)} = 0$ in the steady state and $\mathbf{U} = \mathbf{U}_g = \mathbf{0}$, then Eq. (8) yields $\partial_z(nT) = 0$ and so,

$$\partial_z \ln T = -\partial_z \ln n_2. \quad (40)$$

Here, we have taken into account that $n \simeq n_2$ in the tracer limit. The factor Λ can be written in terms of the diffusion coefficients when one takes into account Eq. (40) and that $j_{1,z}^{(1)} = 0$. Its expression is finally given by

$$\Lambda = \frac{x_1^{-1} D_1^{T*} - D_{11}^* - x_1^{-1} D_{12}^*}{D_{11}^*}, \quad (41)$$

where we have introduced the dimensionless transport coefficients

$$D_{11}^* = \frac{m_1^2 \nu_0}{\rho T} D_{11}, \quad D_{12}^* = \frac{m_1 m_2 \nu_0}{\rho T} D_{12}, \quad D_1^{T*} = \frac{\rho \nu_0}{n T} D_1^T. \quad (42)$$

The explicit dependence of Λ on the parameters of the granular suspension (mass and size ratios, the coefficients of restitution α_{12} and α_{22} , and the dimensionless external temperature T_{ex}^*) can be obtained when one substitutes Eqs. (34) and (35) of D_{11} , D_1^T , and D_{12} , respectively, into Eq. (41). Since $D_{11}^* > 0$, the condition $\Lambda = 0$ is

$$x_1^{-1} D_1^{T*} = D_{11}^* + x_1^{-1} D_{12}^*. \quad (43)$$

Equation (43) gives the marginal segregation curve separating intruder segregation toward the cold wall ($\Lambda > 0$) from intruder segregation toward the hot wall ($\Lambda < 0$). On the other hand, since the number of parameters involved in the segregation problem is still large, it is not easy to disentangle the influence of each mechanism (mass and size ratios, inelasticity in collisions, external temperature, ...) on the intruder segregation problem. Thus, it is convenient first to consider some simple situations.

5.1 Mechanically Equivalent Particles

This is quite trivial case since the system is in fact monodisperse ($m_1 = m_2, \sigma_1 = \sigma_2, \alpha_{11} = \alpha_{22} \equiv \alpha, \gamma_2 = \gamma_1 \equiv \gamma$). In this limit case, $\tau_1 = 1$ and according to Eqs. (34) and (35), $x_1^{-1} D_1^{T*} = 0$ and $D_{11}^* = -x_1^{-1} D_{12}^* = (\nu_D^* + \gamma^*)^{-1}$. Therefore, Eq. (41) yields $\Lambda = 0$ for any value of the coefficients of restitution α_{12} and α_{22} and the bath temperature T_{ex}^* . This implies that no segregation is possible, as expected.

5.2 Elastic Collisions

For elastic collisions ($\alpha_{22} = \alpha_{12} = 1$), $\zeta_0^* = 0, \tau_1 = \theta = 1, \beta = \mu$, and Eq. (43) leads to the condition

$$(\nu_D^* + \gamma_1^*) \frac{\partial \tau_1}{\partial \theta} = 2\gamma_2^* (\mu - 1). \tag{44}$$

Upon deriving Eq. (44), we have considered the region of parameter space where $\nu_D^* + \gamma_1^* - 2\gamma_2^* \neq 0$. It is quite apparent that even for elastic collisions, the segregation criterion ($\Lambda = 0$) is not simple and differs from the simple segregation criterion obtained in the dry case ($\mu = 1$). Figure 3 shows a phase diagram in the $\{m_2/m_1, \sigma_2/\sigma_1\}$ -plane at $T_{ex}^* = 1$. For a given value of the mass ratio m_2/m_1 , it is quite apparent that the region $\Lambda > 0$ (tracer particle falls with respect to excess granular gas) is dominant when the size of gas particles is much larger than that of the tracer particle. This tendency increases with increasing the mass ratio m_2/m_1 .

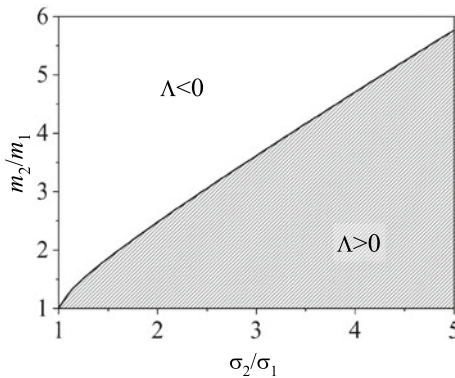


Fig. 3 Plot of the marginal segregation curve ($\Lambda = 0$) for $d = 3, \alpha_{22} = \alpha_{12} = 1$, and $T_{ex}^* = 1$. Points below (above) the curve correspond to $\Lambda > 0$ ($\Lambda < 0$)

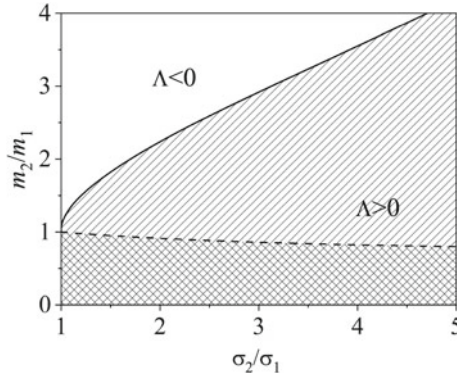


Fig. 4 The same as in Fig. 3 but for $\alpha_{22} = \alpha_{12} = 0.9$. The solid line corresponds to the segregation criterion for granular suspensions while the dashed line refers to the one derived for dry granular mixtures. Points below (above) each curve correspond to $\Lambda > 0$ ($\Lambda < 0$)

5.3 Inelastic Collisions

We consider now the general case where α_{22} and α_{12} are different from 1. In this case, considering the region of parameter space where $\nu_D^* + \gamma_1^* - 2\gamma_2^*\theta^{-1} - \frac{1}{2}\zeta_0^* \neq 0$, Eq. (43) yields

$$\begin{aligned} \left[\nu_D^* + \gamma_1^* - \zeta_0^* + 2\gamma_2^*(\theta^{-1} - 1) \right] \left(\theta \frac{\partial \tau_1}{\partial \theta} - \mu + \tau_1 \right) &= \left(\tau_1 - \mu - 2\lambda_1 \frac{\partial \tau_1}{\partial \lambda_1} \right) \\ &\times \left(\nu_D^* + \gamma_1^* - 2\gamma_2^*\theta^{-1} - \frac{1}{2}\zeta_0^* \right). \end{aligned} \quad (45)$$

This is quite a complex segregation criterion in comparison with the one derived in the dry granular case (no gas phase) where $\Lambda = 0$ if $\mu = \tau_1$ [17, 18]. To illustrate more clearly the differences between both (with and without gas phase) segregation criteria, Fig. 4 shows the marginal segregation curve ($\Lambda = 0$) for the (common) coefficient of restitution 0.9. Figure highlights that the impact of gas phase on tracer segregation is quite significant since, at a given value of the size ratio, the value of the mass ratio m_2/m_1 at which $\Lambda = 0$ is greater in the granular suspension than in the dry granular system. In addition, we also observe that the main effect of gas phase on tracer segregation is to increase the size of the region $\Lambda > 0$ as σ_2/σ_1 increases. This means that the tracer particle attempts to move toward the cold regions as its size decreases with respect to that of the excess granular gas.

6 Concluding Remarks

The primary objective of this short review has been to derive the Navier–Stokes hydrodynamic equations of a binary granular suspension within the context of the inelastic version of the Boltzmann kinetic equation. As usual, the effect of the interstitial surrounding gas on grains has been modeled through an effective external force constituted by a deterministic drag force plus an stochastic Langevin-like force. This way of modeling gas–solid flows is essentially based on the following assumptions and/or simplifications. First, assuming that the granular mixture is rarefied, one supposes that the state of the surrounding gas is not perturbed by the presence of grains and so, it can be treated as a thermostat. Second, the impact of gas phase on collision dynamics is very weak, and consequently, the Boltzmann collision operator is not affected by the presence of the interstitial gas. As a third simplification, one considers the friction coefficients appearing in the thermal-drag forces to be scalar quantities. Finally, as a fourth simplification, one assumes low Reynolds numbers so that only laminar flows are considered.

The road map for obtaining the Navier–Stokes hydrodynamic equations needs to characterize first the homogeneous state. This is important because the Navier–Stokes transport coefficients are obtained from the CE expansion around the above state. Given that the transport coefficients are given in terms of the solutions to a set of coupled linear integral equations, these equations are approximately solved by considering the leading terms in a series expansion of Sonine polynomials. This road map is large and involves many technical steps. Here, for the sake of simplicity, we have obtained the mass flux of a binary granular suspension where the concentration of one of the species is negligible (tracer limit). The tracer limit allows us to provide expressions that are easy to handle for potential applications. In particular, we have briefly analyzed here the thermal diffusion segregation of an intruder or tracer particle in a granular suspension. The segregation criterion obtained here shows significant discrepancies with respect to the one previously derived for dry granular mixtures [17, 18]. These differences between both situations (with and without interstitial gas) are clearly illustrated in Figs. 3 and 4 for elastic and inelastic collisions, respectively.

Multicomponent granular suspensions exhibit a wide range of interesting phenomena for which kinetic theory and hydrodynamics (in the broader sense) may be considered as useful tools for understanding the behavior of such complex materials. However, due to their complexity, many of their features are not still completely understood. For this reason, from the theoretical side, one has to introduce new ingredients in the model for approaching more realistic situations. In this context, the extension of the results presented in this review to inertial suspensions of inelastic rough hard spheres could be an interesting and challenging problem in the near future.

Acknowledgements The present work has been supported by the Spanish Government through Grant No. PID2020-112936GB-I00 funded by MCIN/AEI/10.13039/501100011033 and by the Junta de Extremadura (Spain) Grant Nos. IB20079 and GR18079, partially financed by “Fondo

Europeo de Desarrollo Regional” funds. The research of Rubén Gómez González has been also supported by the predoctoral fellowship BES-2017-079725 from the Spanish Government.

References

1. See for instance, M.E. Möbius, B.E. Lauderdale, S.R. Nagel, H.M. Jaeger, Brazil-nut effect: size separation of granular particles. *Nature* **414**, 270 (2001); P. Sánchez, M.R. Swift, P.J. King, Stripe formation in granular mixtures due to the differential influence of drag. *Phys. Rev. Lett.* **93**, 184302 (2004); J.C. Pastenes, J.C. Géminard, F. Melo, Interstitial gas effect on vibrated granular columns. *Phys. Rev. E* **89**, 062205 (2014)
2. D.L. Koch, R.J. Hill, Inertial effects in suspensions and porous-media flows. *Annu. Rev. Fluid Mech.* **33**, 619 (2001)
3. N.V. Brilliantov, T. Pöschel, *Kinetic Theory of Granular Gases* (Oxford University Press, Oxford, 2004)
4. V. Garzó, *Granular Gaseous Flows* (Springer Nature, Cham, 2019)
5. J.J. Brey, J.W. Dufty, C.S. Kim, A. Santos, Hydrodynamics for granular flow at low-density. *Phys. Rev. E* **58**, 4638 (1998)
6. V. Garzó, J.W. Dufty, Dense fluid transport for inelastic hard spheres. *Phys. Rev. E* **59**, 5895 (1999); V. Garzó, J.W. Dufty, Hydrodynamics for a granular binary mixture at low density. *Phys. Fluids* **14**, 1476 (2002); V. Garzó, J.W. Dufty, C.M. Hrenya, Enskog kinetic theory for polydisperse granular mixtures. I. Navier–Stokes order transport. *Phys. Rev. E* **76**, 031303 (2007); V. Garzó, C.M. Hrenya, J.W. Dufty, Enskog kinetic theory for polydisperse granular mixtures. II. Sonine polynomial approximation. *Phys. Rev. E* **76**, 031304 (2007)
7. N. Khalil, V. Garzó, Transport coefficients for driven granular mixtures at low-density. *Phys. Rev. E* **88**, 052201 (2013)
8. R. Gómez González, N. Khalil, V. Garzó, Enskog kinetic theory for multicomponent granular suspensions. *Phys. Rev. E* **101**, 012904 (2020)
9. S. Chapman, T.G. Cowling, *The Mathematical Theory of Nonuniform Gases* (Cambridge University Press, Cambridge, 1970)
10. X. Yin, S. Sundaresan, Fluid-particle drag in low-Reynolds-number polydisperse gas-solid suspensions. *AIChE J.* **55**, 1352 (2009)
11. See for instance, J.M. Montanero, V. Garzó, Monte Carlo simulation of the homogeneous cooling state for a granular mixture. *Granular Matter* **4**, 17 (2002); S.R. Dahl, C.M. Hrenya, V. Garzó, J.W. Dufty, Kinetic temperatures for a granular mixture. *Phys. Rev. E* **66**, 041301 (2002); A. Barrat, E. Trizac, Molecular dynamics simulations of vibrated granular gases. *Phys. Rev.* **66**, 051303 (2002); P. Krouskop, J. Talbot, Mass and size effects in three-dimensional vibrofluidized granular mixtures. *Phys. Rev. E* **68**, 021304 (2003); M. Schröter, S. Ulrich, J. Kreft, J.B. Swift, H.L. Swinney, Mechanisms in the size segregation of a binary granular mixture. *Phys. Rev. E* **74**, 011307 (2006)
12. R.D. Wildman, D.J. Parker, Coexistence of two granular temperatures in binary vibrofluidized beds. *Phys. Rev. Lett.* **88**, 064301 (2002); K. Feitosa, N. Menon, Breakdown of energy equipartition in a 2D binary vibrated granular gas. *Phys. Rev. Lett.* **88**, 198301 (2002)
13. G.A. Bird, *Molecular Gas Dynamics and the Direct Simulation of Gas Flows* (Oxford University Press, Oxford, 1994)
14. N. Brilliantov, T. Pöschel, Hydrodynamics and transport coefficients for dilute granular gases. *Phys. Rev. E* **67**, 061304 (2003)
15. N. Khalil, V. Garzó, Homogeneous states in driven granular mixtures: Enskog kinetic theory versus molecular dynamics simulations. *J. Chem. Phys.* **140**, 164901 (2014)
16. J. Kincaid, E.G.D. Cohen, M. López de Haro, The Enskog theory for multicomponent mixtures. IV. Thermal diffusion. *J. Chem. Phys.* **86**, 963 (1987)

17. J.J. Brey, M.J. Ruiz-Montero, F. Moreno, Energy partition and segregation for an intruder in a vibrated granular system under gravity. *Phys. Rev. Lett.* **95**, 098001 (2005)
18. V. Garzó, Segregation in granular binary mixtures: thermal diffusion. *Europhys. Lett.* **75**, 521–527 (2006)